

Mechanical Characterization of Sol-Gel Coatings Using KLA Nano Indenter systems



Introduction

This application note presents the results of nanomechanical tests in which a KLA Nano Indenter system was used to measure the Young's modulus and hardness of three sol-gel coatings. The same instrument was also utilized to perform controlled scratch tests to evaluate adhesion. The samples provided for testing are described in Table 1.

Indentation Tests

Twenty indentation tests were performed on each sample using a KLA Nano Indenter system with a standard load transducer fitted with a Berkovich indenter tip. The Continuous Stiffness Measurement (CSM) option was used to measure properties as a continuous function of penetration depth.

Figure 1 shows a typical load-time history for a single test. Each indentation test consists of the following test segments:

1. Approach the surface until contact is detected.
2. Load such that the loading rate divided by the load remains constant at 0.5/sec until the penetration depth reaches 3000nm (3 μ m).
3. Hold the peak force constant for 10 seconds.
4. Reduce the force on the indenter until the applied force becomes 10% of the peak force.
5. Hold the force on the indenter constant for 100 seconds.
6. Withdraw the indenter completely.

Reference	Description	Thickness (μ m)	Substrate
AG5T5R82	50% organic, 50% inorganic	6 \pm 1	aluminum
AG5T5R111	50% organic, 50% inorganic	12 \pm 1	aluminum
VR82	50% organic, 50% inorganic	6 \pm 1	glass

Table 1. Samples for testing.

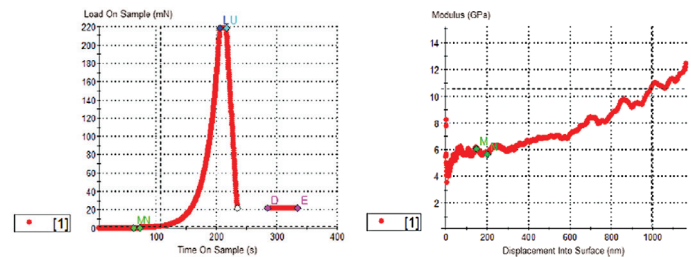


Figure 1. Example of load-time history for a single indentation test. (Note: since loading terminated at a prescribed displacement, peak forces varied from test to test.)

Figure 2. Data analysis: Young's modulus for this test on this film is calculated as the average of all values between the markers M and N. The positions of markers M and N are controlled by the user.

The loading process causes a constant strain rate to be applied to the test material, which is necessary when testing materials for which the measured hardness depends on strain rate. Let us consider a bulk sample (not a thin film) of strain-rate-sensitive material. Only a loading process that holds P'/P constant will return a hardness that is constant with penetration depth. Indentation tests that hold the loading rate or displacement rate constant will measure a hardness that appears to decrease with indentation depth, even on a bulk sample with uniform properties. This is because the imposed strain rate is decreasing.¹

The fifth test segment evaluates the change in displacement due to thermal expansion and/or contraction of the sample and/or instrument. Data acquired in the last 50 seconds of this test segment are used to calculate a thermal drift rate, which is then used to make a small correction to displacements measured throughout the test. This common procedure is explained in more detail elsewhere.²

The CSM option works by imposing a small oscillation on the indenter during loading. Typically, the amplitude of the force oscillation is controlled (increased) such that the amplitude of the displacement oscillation remains constant at 2nm. The amplitude of the force oscillation relative to the amplitude of the displacement oscillation allows one to calculate stiffness as a continuous function of penetration depth. This, in turn, enables

the calculation of Young’s modulus and hardness as a continuous function of indentation depth.³

Therefore, each indentation test returns Young’s modulus and hardness as a function of indentation depth. The properties of the film alone are calculated by averaging over an appropriate displacement range — for these films, the range was set to 150–200nm. For example, the measured modulus from the first test on sample AG5T5R82 is shown in Figure 2. The value of Young’s modulus for this test, E1, is reported as the average of all data between the markers M and N. The same procedure is repeated for every test to get E2, E3, etc.

Finally, we calculate an average and standard deviation for all n valid tests to get

$$\sigma(\bar{E}) = \sqrt{\frac{1}{n} \sum_{i=1}^n (E_n - \bar{E})^2}$$

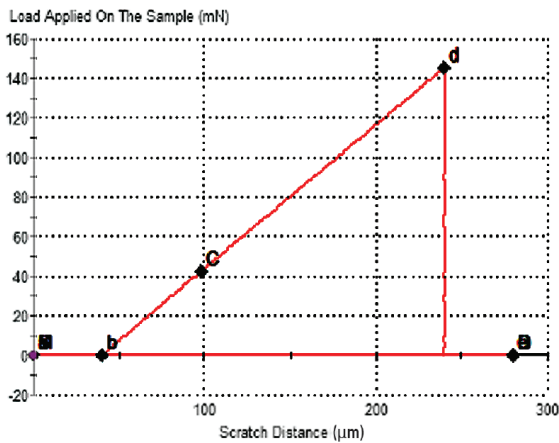


Figure 3. Applied force as a function of scratch distance for a single scratch test.

To simplify the presentation of properties as a function of penetration depth (and to facilitate comparison among samples), we also average the channels of Young’s modulus and hardness into small, discrete displacement windows. For example, for sample AG5T5R82, we take all data from all valid tests for which the penetration depth is between 0nm and 5nm and report a single average and standard deviation for this window. Then we take all data from all valid tests for which the penetration depth is between 5nm and 10nm and report an average and standard deviation for this window, etc. The traces in Figure 6 were generated in this way.

Scratch Tests

Six scratch tests were performed on each sample. Lateral forces were not measured, so the Lateral Force Measurement (LFM) option is not necessary for duplication of this work, although it may be advantageous for future testing while using Nano Indenter G200. Figure 3 shows the applied force as a function of scratch position. Each scratch test consists of the following test segments:

1. A first profile of the surface is realized under a very small load (100µN), in order to have the original morphology of the surface before the scratch.
2. Then, along the same path, the normal load is increased from 0mN to 150mN over a distance of 200 microns.
3. A final profile is realized under a very small load (100µN) to measure the residual deformation in the groove.

If the scratch causes failure in the material, the “critical load” is calculated as the load corresponding to the position at which the final scan reveals a significant increase in roughness. In other words, if the final scan (segment 3) reveals a significant increase in roughness at a position of 98 microns from the origin of the scratch, then the critical load is taken to be the load that was applied during the scratch (i.e., during segment 2) at that same position.

Results – Indentation

Table 2 summarizes the film properties measured in this work. Images of residual impressions are provided in Figure 4. Sample VR82 exhibited adhesive failure, as evidenced by a “halo” around the residual impression. The point of failure is clear in the indentation data as illustrated in Figure 5. This failure occurred at an applied force of 87.5mN ± 11.8mN. The two samples on aluminum substrates did not exhibit this failure.

Sample	E Average Over Defined Range	σ(E)	H Average Over Defined Range	σ(H)	n
	GPa	GPa	GPa	GPa	
AG5T5R82	6.24	0.18	0.515	0.014	20
AG5T5R111	5.68	0.10	0.514	0.016	16
VR82	5.66	0.07	0.442	0.009	19

Table 2. Summary of sol-gel film properties.

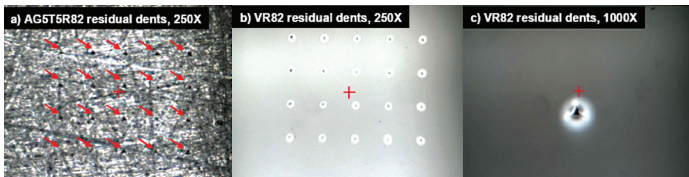


Figure 4. Residual impressions. The “halo” around VR82 dents indicates fracture at the interface.

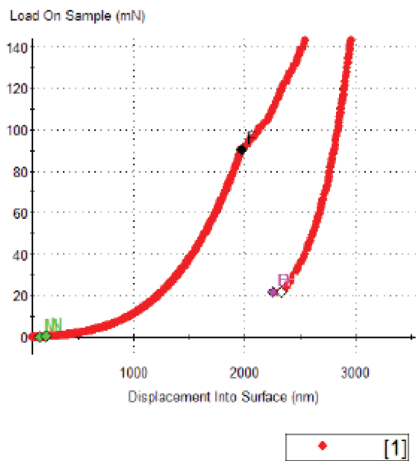


Figure 5. Example of adhesive failure during an indentation test on VR82. Point of failure, F, was identified automatically.

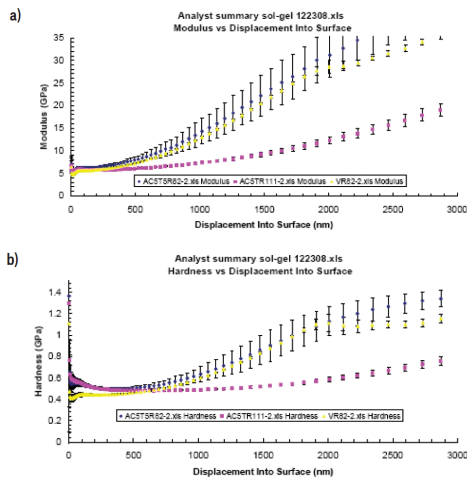


Figure 6. Properties of sol-gel films as a function of penetration depth.

Results – Scratch

Sample VR82 also failed during scratch testing. The critical load at failure was $43.7\text{mN} \pm 1.2\text{mN}$. This is much lower than the load causing failure during indentation, probably because lateral forces contributed to the failure. Neither of the coatings on aluminum substrates exhibited failure during scratch testing. Figure 8 shows the residual scratches on sample VR82.

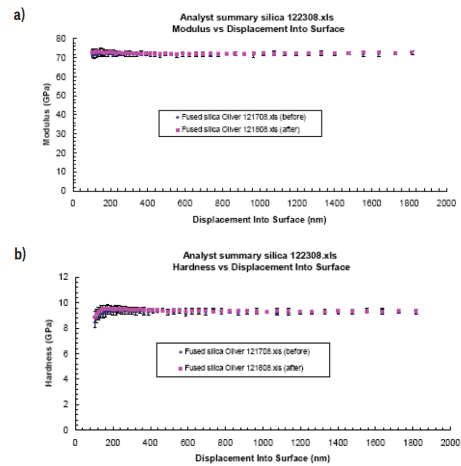


Figure 7. Properties of fused silica reference material, before and after testing sol-gel samples.

Figure 6 shows the evolution of hardness and modulus as a function of penetration depth for all samples. Finally, Figure 7 shows corresponding results for the fused silica tested as a reference material immediately before and after the sol-gel samples.

Discussion and Conclusions

Indentation tests to measure Young’s modulus and hardness were prescribed to go to a maximum depth of 3000nm (3µm). After reviewing the resulting traces of modulus and hardness as a function of displacement, the displacement range of 150–200nm was selected for reporting film properties. The lower limit of this range, 150nm, was sufficiently deep to get past “surface effects”, whereas the upper limit was sufficiently shallow to avoid significant influence from the substrate. On future testing of similar samples, it would be better experimental practice to limit the depth of the test to something only a little greater than the upper limit of the range that will be used to report properties. Limiting the indentation depth to something like 250nm would minimize the influence of thermal drift on the results.

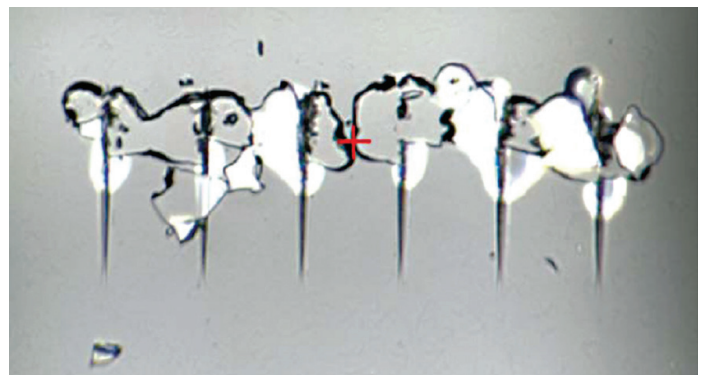


Figure 8. Residual scratches on sample VR82.

Only the sol-gel film on the glass substrate (sample VR82) exhibited adhesive failure. This is probably due to the fact that the rougher aluminum substrate provided a substantially greater surface area available for bonding between the film and substrate. The diameter of the “halo” around the residual indents can be used to calculate interfacial fracture toughness. The fact that the normal load causing failure was much lower for scratch testing is not surprising, because lateral forces probably contribute to the failure. Although the LFM option was not used in this testing, it may be used to measure the lateral force on the indenter during scratching.

We were not expecting sample VR82 to fail during indentation; however, when failure was evident, NanoSuite Explorer software was utilized to quickly define an algorithm that would automatically pick out the critical indentation load identified by point F in Figure 5.

Technology and Applications

The KLA Nano Indenter systems are powered by electromagnetic actuation to achieve dynamic range in force and displacement. The instrument’s design avoids lateral displacement artifacts, while software compensates fully for any drift in force. Using KLA Nano Indenters, researchers can measure Young’s modulus

and hardness in compliance with ISO 14577. Deformation can be measured over six orders of magnitude (from nanometers to millimeters).

Applications of the KLA Nano Indenter systems include semiconductor, thin films, and MEMs (wafer applications); hard coatings and DLC (diamond-like carbon) films; composite materials, fibers and polymers; metals and ceramics; and biomaterials.

References

1. B.N. Lucas and W.C. Oliver, “Indentation power-law creep of high-purity indium”, *Metallurgical and Materials Transactions A*, 30 (3), 601-610 (1999).
2. J.L. Hay and G.M. Pharr, “Instrumented Indentation Testing”, book chapter in *ASM Handbook Volume 8: Mechanical Testing and Evaluation* (10th edition), edited by H. Kuhn and D. Medlin, pp. 232-243, ASM International, Materials Park, OH (2000).
3. W.C. Oliver and G.M. Pharr, “An Improved Technique for Determining Hardness and Elastic Modulus Using Load and Displacement Sensing Indentation Experiments”, *Journal of Materials Research*, Volume 7, Issue 6, pp. 1564-1583 (1992).

KLA SUPPORT

Maintaining system productivity is an integral part of KLA’s yield optimization solution. Efforts in this area include system maintenance, global supply chain management, cost reduction and obsolescence mitigation, system relocation, performance and productivity enhancements, and certified tool resale.

© 2019 KLA Corporation. All brands or product names may be trademarks of their respective companies. KLA reserves the right to change the hardware and/or software specifications without notice.

KLA Corporation
One Technology Drive
Milpitas, CA 95035
www.kla.com

Printed in the USA
2019-01